On the reactivity of Mo species for methane partial oxidation on Mo/HMCM-22 catalysts

Shaojun Miao[1], Lin Liu[1], Yuxiang Lian[1], Xiangxue Zhu[2], Shutian Zhou[1], Yan Wang[1], and Xinhe Bao[1,*]

[1]*State Key Laboratory of Catalysis, Dalian Institute of Chemical Physics, CAS, 457 Zhongshan Road, P.O. Box 110, Dalian 116023, P.R. China*
[2]*Natural Gas Utilization and Applied Catalysis Laboratory, Dalian Institute of Chemical Physics, CAS, 457 Zhongshan Road, P.O. Box 110, Dalian 116023, P. R. China*

Received 3 May 2004; accepted 19 July 2004

By characterizing fresh and used Mo/HMCM-22 catalysts with ICP–AES, XRD, NH_3-TPD technique, UV–Vis DRS and UV Raman spectroscopy, the reactivity of Mo species for methane partial oxidation into formaldehyde were directly studied with a new point of view. By comparing the fresh and used catalysts, it was found that the tetrahedral Mo species bonding chemically to the support surface were practically unchanged after the reaction, while the polymolybdate octahedral Mo species, which had a rather weak interaction with the MCM-22 zeolite, leached out during the reaction, especially when the Mo loading was high. Correspondingly, it was found from the time-on-stream reaction data that the HCHO yield remained unchanged, while CO_x decreased with the reaction time during the reaction. By combining the characterization results and the reaction data, it can be drawn that the isolated tetrahedral molybdenum oxo-species (T_d) is responsible for HCHO formation, while the octahedral polyoxomolybdate species (O_h) will lead to the total oxidation of methane.

KEY WORDS: methane partial oxidation; formaldehyde; Mo/HMCM-22; tetrahedral molybdate; octahedral polyoxomolybdate.

1. Introduction

The direct conversion of methane to oxygenates such as methanol and formaldehyde has attracted significant interest in the field of chemical engineering and catalysis for decades due to the considerable increase in the world-wide natural gas reserves [1–3]. Several supported oxide catalysts have been employed for this reaction at atmospheric pressure, among them are the supported MoO_3 catalysts, which have been reported to be one of the most active and selective ones for oxygenate production [4–13]. Silica as a support has been widely used in metal oxide catalysts for methane partial oxidation, and a number of papers have illustrated that silica itself shows discernible activity for formaldehyde formation [14–16].

The partial oxidation of methane to oxygenates over silica supported MoO_3 catalysts has been studied extensively. The most recent papers concerning the catalysts for the title reaction have been focused on the elucidation of the relationship between the structure of the supported metal oxide phase and their role in the reaction mechanism. Smith and Ozkan [7] have examined the partial oxidation of methane to formaldehyde over MoO_3/SiO_2, investigated the surface species formed on the support and their effect on reactivity and selectivity [17]. They found that at low Mo loadings, the predominant species was a silicomolybdic species with terminal Mo = O sites. However, at higher loadings, polymolybdate species with Mo–O–Mo bridges began to form at the expense of Mo = O sites. The silicomolybdic species with terminal Mo–O sites were found to have better selectivity for HCHO than the polymolybdate species with Mo–O–Mo bridging sites.

Lucas *et al.* [10] have studied the partial oxidation of methane over Mo/ZSM-5 catalysts to demonstrate the specificity of the monomeric molybdenum oxo-species in the production of formaldehyde from methane [10]. Two series of Mo/ZSM-5 catalysts were prepared. The second series was obtained by washing the catalysts of the first series, which was prepared by conventional aqueous impregnation method, with ammonia aqueous solution to remove the physically adsorbed molybdenum species. By means of XRD, UV–Vis, and TPR techniques and combined with catalytic results of methane partial oxidation, the authors showed that the Mo = O sites of monomeric species were responsible for HCHO production.

The early investigators have tried to reduce the amount of Mo–O–Mo sites by decreasing Mo loading or washing with ammonium aqueous solution in order to explore the specificity of Mo species in methane partial oxidation. However, it is easy to see that with these methods not only the polymolybdate species but also the isolated tetrahedral Mo species would be lowered, so that the intention in clarifying the specificity of isolated Mo species for HCHO forming would be difficult to achieve. In this study, by employing Mo/HMCM-22 as the catalyst samples, which have been extensively and

*To whom correspondence should be addressed.
E-mail: xhbao@dicp.ac.cn

1011-372X/04/0900–0209/0 © 2004 Plenum Publishing Corporation

systematically studied in our lab [18–20], we tried to study the reactivity of Mo species for methane partial oxidation into formaldehyde from a new point of view. Instead of changing the amount of polymolybdate species in the catalyst preparation step, we characterized the Mo species in the fresh and used catalysts. Then, by combining the results with the time-on-stream reaction data, the reactivity of Mo species for methane partial oxidation into formaldehyde could be elucidated directly and clearly.

2. Experimental

2.1. Catalyst preparation

MCM-22 zeolite was synthesized according to the procedures described in refs. [21,22] using hexamethyleneimine (HMI) as the structure directing agent. The ratio of SiO_2 to Al_2O_3 of the MCM-22 was about 20. The MCM-22 zeolites synthesized by us exhibit a typical MCM-22 crystalline structure (MWW), as evidenced by XRD determinations (D/Max-RB diffractometer using Cu Kα radiation), and no hybrid crystallites were observed.

MoO_3/HMCM-22 catalysts were prepared by incipient wetness impregnation method and denoted as xMo/HMCM-22, where x was the nominal Mo content by weight. Thus, 5 g of HMCM-22 powder was impregnated with 5 mL of aqueous solution containing the desirable amount of ammonium heptamolybdate (AHM), and then dried at room temperature for 12 h. After further dried at 373 K for 8 h and calcined in air at 773 K for 5 h, the samples were crushed and sieved to 40–60 mesh granules for catalytic evaluations.

2.2. Catalyst characterization

The MoO_3 loading on the catalysts was analyzed with IRIS Advantage ICP–AES instrument (TJA Co., USA).

X-ray powder diffraction patterns were recorded with a D/Max-RB diffractometer using Cu Kα radiation at room temperature, with instrumental settings of 40 kV and 100 mA. The powder diffractograms of the samples were recorded from 5 ° to 40 ° at a 5 °/min scanning rate.

UV–Vis diffuse reflectance spectra (UV–Vis DRS) were recorded on a JASCO V-550 UV-Visible spectrophotometer. The scanning wavelength range was 190–800 nm and the scanning speed was 100 nm/min.

UV resonance Raman spectra were obtained on a homemade UV resonance Raman spectrometer. A 244.0 nm line from an Innova 300 FRED laser and a 325 nm line of a He–Cd laser were used as the excitation sources.

NH_3 temperature-programmed desorption (NH_3-TPD) was performed on a conventional setup equipped with a thermal conductivity detector. About 0.14 mg of the sample was first flushed with He (30 mL/min) at 873 K for 30 min, then cooled to 423 K and saturated with NH_3 until equilibrium. It was then flushed with He again until the baseline of the integrator was stable. NH_3-TPD was then promptly started from 423 to 973 K at 15 K/min. All profiles were deconvoluted into three or four peaks by the Gaussian and Lorentzian curve-fitting method.

2.3. Catalytic evaluation

The reactions were carried out in a fixed-bed continuous-flow reactor made of quartz (100× 2 mm o.d.) which was connected to a small tube so that the products could be rapidly removed from the heated zone. The reactor was heated by an external oven. A small glass tube containing a thermocouple was placed in the middle of the catalyst bed. Generally 0.2 g of catalyst sample was used. The dead volume of the reactor was filled with quartz beads. The typical reacting gas mixture consisted of $He/CH_4/O_2 = 3/2/1$. The flow rate of the reactants was usually 60 mL/min and the space velocity was 18,000 L/kg h. The products were analyzed by an online gas chromatography (Agilent 6890N) equipped with a thermal conductivity detector.

3. Results and discussion

3.1. Catalysts characterization by XRD

Figure 1 shows the XRD patterns of MCM-22 without Mo addition and with different Mo loadings. The X-ray diffraction pattern of the as-synthesized MCM-22 sample shows almost the same feather as described in references [21–24]. After addition of MoO_3, the corresponding patterns display only the characteristic peaks of MCM-22, and no MoO_3 crystallite

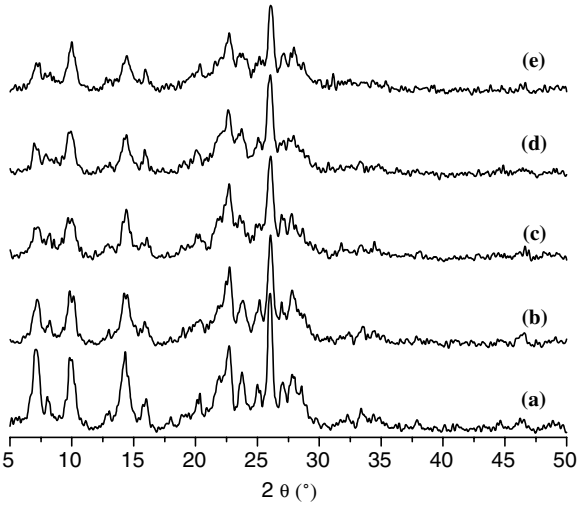

Figure 1. XRD patterns of Mo/MCM-22 catalysts with different molybdenum loading:(a) HMCM-22; (b) 1%Mo/MCM-22; (c) 2%Mo/MCM-22; (d) 4%Mo/MCM-22; (e) 8%Mo/MCM-22.

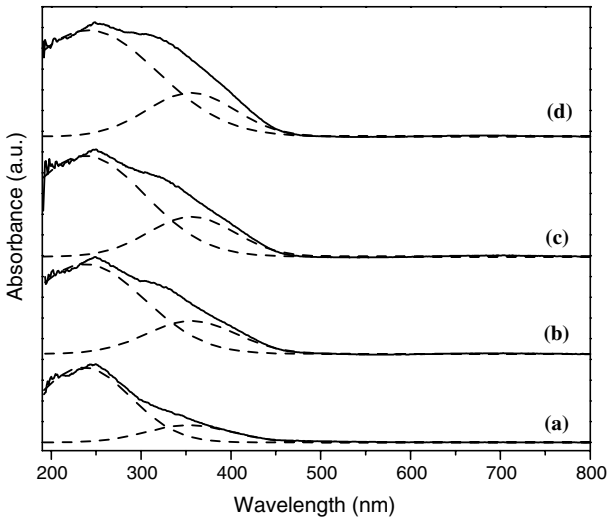

Figure 2. UV–Vis diffuse reflectance spectra of Mo/MCM-22 with different molybdenum loading:(a) 1%Mo/MCM-22; (b) 2%Mo/MCM-22; (c) 4%Mo/MCM-22; (d) 8%Mo/MCM-22.

patterns were observed even for a Mo loading as high as 8%. On the other hand, the crystallinity of the MCM-22 zeolite decreased slightly with the increasing of Mo loading, as revealed by the X-ray patterns. This indicates that MoO_3 was highly dispersed on the surface of MCM-22 and/or in its channels.

3.2. Characterization of the supported molybdate species

In figure 2 the UV–Vis diffuse reflectance spectra of the Mo/MCM-22 catalysts with different molybdenum loadings are presented. For all of the samples their spectra consist of two overlapping bands at about 250 and 350 nm after curve fitting. According to the reported wavelength for oxomolybdenum species [25–28], the band at 250 nm could be assigned to isolated tetrahedrally coordinated Mo(VI) species ($Mo(T_d)$) while the other band at about 350 nm could be assigned to octahedral polyoxomolybdate Mo(VI) ($Mo(O_h)$) species. Figure 2 also shows that the amount of both of these Mo species on the Mo/MCM-22 catalysts increased with the increasing of the Mo loading, but $Mo(O_h)$ species increased more notably than the $Mo(T_d)$. However, due to the broad nature of the UV bands, there is not enough evidence to discard the presence of a crystalline MoO_3 phase in the Mo/MCM-22 samples. As indicated by the XRD results, no MoO_3 crystallite patterns were observed even for a Mo loading as high as 8%. Thus, it can be concluded that only the $Mo(T_d)$ and $Mo(O_h)$ species were present on the surface of the catalysts in this study.

3.3. Methane oxidation

The reaction of partial oxidation of methane with molecular oxygen over Mo/MCM-22 catalysts can lead to the formation of HCHO, CO, CO_2 and H_2O. Prior to the catalytic activity measurements, the contributions of gas-phase reaction and reactor wall reaction were evaluated by performing a series of experiments with the empty reactor packed with quartz wools. In the absence of a catalyst and at the temperatures and flow rates employed in the present work, conversion of methane and selectivities to methanol and formaldehyde were all negligible. Thus, the observations in the presence of catalysts were primarily the results of heterogeneous catalytic process, with very little or no intrusion of pure gas-phase reactions and reactor wall effect.

Table 1 lists the catalytic results over pure HMCM-22 as well as Mo/MCM-22 with different Mo loading. The data at each temperature listed in the table are the average of three sampling measurements after at least 1 h of time on stream at the given temperature. It can be seen that even without Mo modifying, HMCM-22 shows significant activity for methane conversion, although most methane is converted into CO_x.

Compared with pure HMCM-22, it was observed that the methane conversion and HCHO selectivity were apparently improved when a certain amount of Mo was loaded on the HMCM-22. The result confirmed the positive effect of Mo species on methane conversion to formaldehyde. Further increasing of the Mo loading, however, would somewhat diminish methane conversion, which was in agreement with the results over Mo/HZSM-5 catalysts [10]. The reason might be that a certain amount of the Mo species could cooperated with Brønsted acid sites to form active centers for methane activation and HCHO production, while too much Mo species would destroy the acidic sites and thus lower the activity. It was also observed that methane conversion was increased with the raising of the reaction temperature. Moreover, the HCHO selectivity increased with the temperature when the Mo loading was low (1%), but decreased at higher Mo loading (2–8%).

The changes in CH_4 conversion and the products yields with on-stream time on the 1%Mo/MCM-22 and 8%Mo/MCM-22 catalysts are shown in figures 3 and 4. It was found that the methane conversion and CO_x yield reached a maximum at the beginning of the reaction, and decreased with the reaction time. After running for 12 h, the methane conversion and CO_x yield decreased from 5.9% and 132.4 mol/kg h to 4.7% and 103.9 mol/kg h, respectively. Meanwhile, it is interesting to find that HCHO yield was remained constant during the whole reaction period (ca. 12.2 mol/kg h). The same results was obtained for 8%Mo/MCM-22 catalyst, but the decrease in methane conversion and CO_x yield was much sharper, i.e., from 5.9% and 134.7 mol/kg h to 1.8% and 34.6 mol/kg h, respectively.

Besides above, it should be pointed out that the formaldehyde space-time yield obtained on Mo/MCM-22 catalysts in this work were better than those reported by Lucas *et al.* [10] and comparable to those obtained for MoO_3/SiO_2 catalysts.

Table 1
Methane conversion and product selectivities for methane partial oxidation over unpromoted HMCM-22 and Mo modified MCM-22 catalysts series[a]

Catalyst	T(°C)	CH_4 Conv. (%)	Selectivity (%)			STY [b] $_{HCHO}$ (mol/kg h)
			HCHO	CO	CO_2	
HMCM22	500	0.78	8.4	22.8	68.7	1.6
	550	1.19	4.4	20.3	75.3	1.3
	600	2	4.8	26.5	68.7	2.3
	650	4.31	6.2	38.3	55.5	6.5
1%Mo/MCM22	500	0.57	7.8	79.7	12.5	1.1
	550	0.88	8.8	79.3	11.9	1.9
	600	2.21	10.3	77.9	11.8	5.6
	650	6.26	7.6	85.8	12	11.6
2%Mo/MCM22	500	0.49	11.4	48.4	40.2	1.4
	550	0.96	10.5	46.9	42.7	2.5
	600	2.49	7.7	46.3	46	4.7
	650	6	5.7	50	44.3	8.3
4%Mo/MCM22	500	0.4	12.2	79.4	8.3	1.2
	550	0.8	11.4	81.5	7.1	2.2
	600	2.11	10.1	82.2	7.7	5.2
	650	4.87	9.4	82	8.6	11.2
8%Mo/MCM22	500	0.43	13.8	78	8.2	1.5
	550	0.77	12	81.3	6.7	2.3
	600	1.96	10.8	81.2	8	5.2
	650	3.8	12.2	78.9	8.9	11.3

[a]Reaction conditions: W/F = 1.24 g h mol^{-1}; molar ratio CH_4/O_2 = 2.
[b]Formaldehyde space–time yield.

3.4. Comparison of the fresh and used Mo/MCM-22 catalyst

Figure 5 compares the XRD patterns of the fresh 8%Mo/MCM-22 and the catalyst after 12 h of time on stream for CH_4 partial oxidation (denoted as "used"). There was no obvious difference between the fresh and used samples. These results indicated that the Mo species did not undergo aggregation into MoO_3 crystallines during the reaction process.

The contents of Mo in the fresh and used 8%Mo/MCM-22 catalysts were detected by ICP–AES technique. The Mo content of the fresh catalyst is 7.1% and that of the used one is 6%. It is obvious that some molybdenum species were leached out during methane partial oxidation at 650 °C.

Figures 6 and 7 list the UV–Vis spectra of the fresh and used Mo/MCM-22 catalysts with Mo loading of 1% and 8%, respectively. In order to distinguish different surface Mo species, the spectra were also deconvoluted

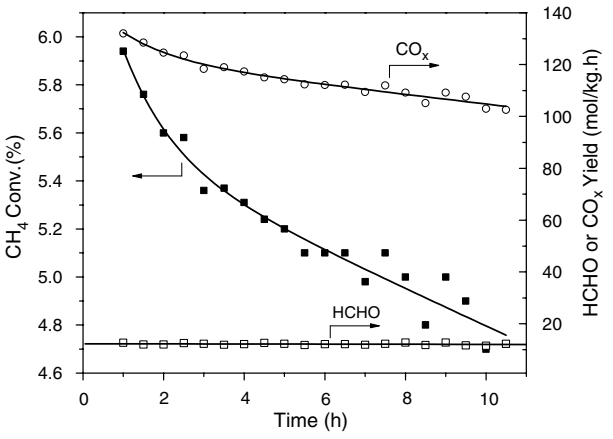

Figure 3. Changes of the methane conversion and the yields of HCHO and CO_x with the time on stream on the 1%Mo/MCM-22 catalyst.

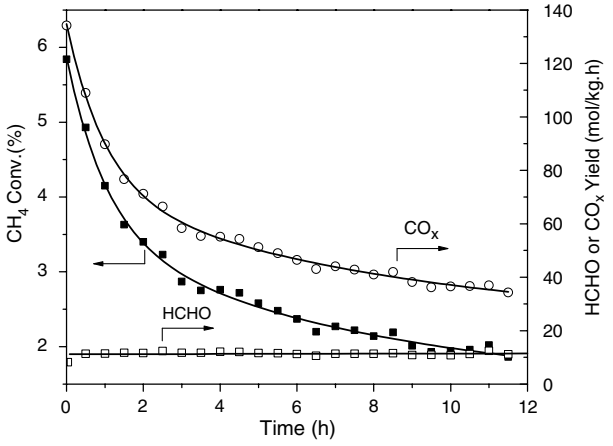

Figure 4. Changes of the methane conversion and the yields of HCHO and CO_x with the time on stream on the 8%Mo/MCM-22 catalyst.

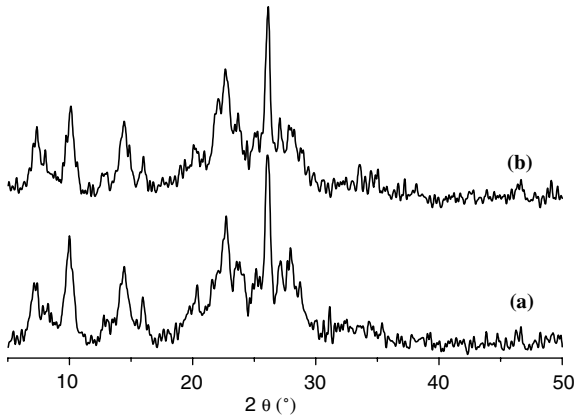

Figure 5. Comparison of XRD patterns: (a) fresh and (b) used 8%Mo/MCM-22 catalysts.

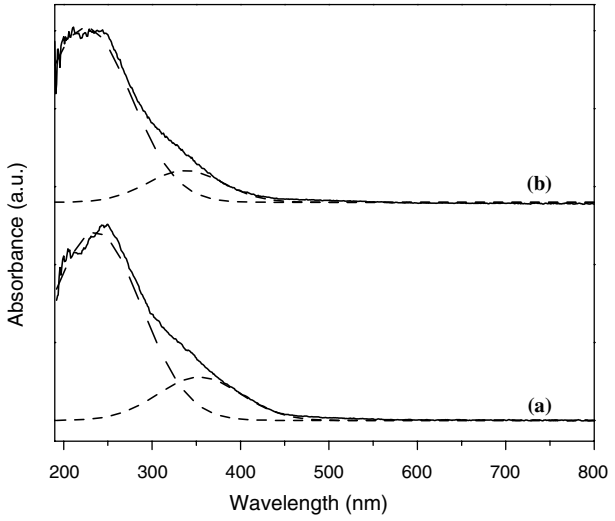

Figure 6. UV diffuse reflectance spectra: (a) fresh and (b) used 1%Mo/MCM-22 catalysts.

into two Gaussian curves, which were assigned to isolated tetrahedrally coordinated Mo(VI) species and octahedral polyoxomolybdate Mo(VI) species. The absorption band and intensity of the deconvoluted curves are summarized in table 2. By comparing the UV–Vis spetra of the fresh and used Mo/MCM-22 catalysts, it is obvious that the absorption band and intensity of the Mo^{6+} (T_d) remained practically unchanged, while the absorption band of the Mo^{6+} (O_h) shifted slightly to low wavelength, and its absorption intensity dropped remarkably, especially for the catalyst with 8% Mo loading. Based on the above ICP–AES analysis, conclusion could be drawn that the leached Mo species were from the octahedral polyoxomolybdate Mo(VI) species.

UV Raman spectroscopy was a useful tool for characterizing supported Mo species owing to not only the avoidance of fluorescence but also the resonance Raman enhancement [30]. Two lasers were employed as

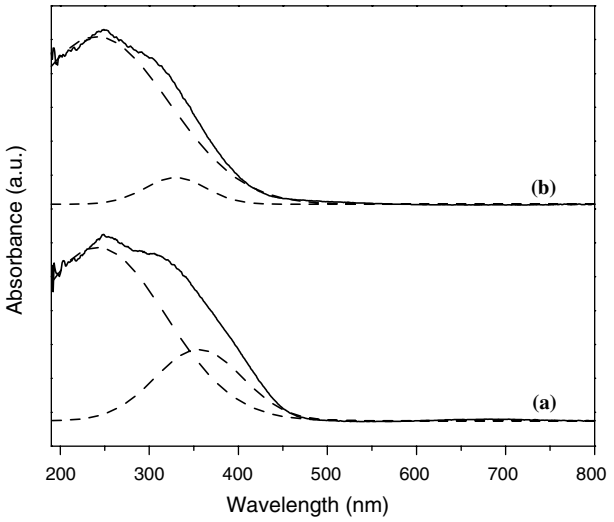

Figure 7. UV diffuse reflectance spectra: (a) fresh and (b) used 8%Mo/MCM-22 catalysts.

Table 2
UV–Vis spectra of the fresh and used 1% and 8% Mo/MCM22 catalysts

Sample	Low		High	
	Wavelength (nm)	Intensity (a.u.)	Wavelength (nm)	Intensity (a.u.)
1%				
Fresh	233.2	47.2	356.9	9.8
Used	225.4	45	337.8	6.6
8%				
Fresh	242.6	98.7	356.2	25.9
Used	241.7	101.1	334.7	6.8

the exciting source on the basis of the results of UV–Vis DRS. When the laser at 244 nm, which is close to the UV–Vis DRS band at 240 nm, was employed as the exciting source, the resonance Raman effect enhanced the Raman bands at 988 cm^{-1} (stretching vibration of Mo = O), which was attributed to the tetrahedral molybdate species. On the other hand, when the laser of 325 nm, which was close to the band at 350 nm, was used, the Raman band at 820 cm^{-1} (asymmetric vibration of Mo–O–Mo) due to the octahedral polyoxomolybdate species was enhanced. From the UV Raman spectra of the fresh catalyst, it is obvious that 988 (figure 8(a)) and 820 cm^{-1} (figure 8(b)) bands could be clearly observed, which means both isolated tetrahedral molybdate species and octahedral polyoxomolybdate species were supported on the surface of the MCM-22, which was in accorded with the results of UV–Vis spectra. After running the reaction of CH_4 partial oxidation for 12 h, however, the band at 820 cm^{-1} was decreased significantly (figure 8(b)), while the band at 988 cm^{-1} practically remained unchanged (figure 8(a)). These results further confirmed the findings by the UV–Vis diffuse reflectance spectrometry, namely, some of the

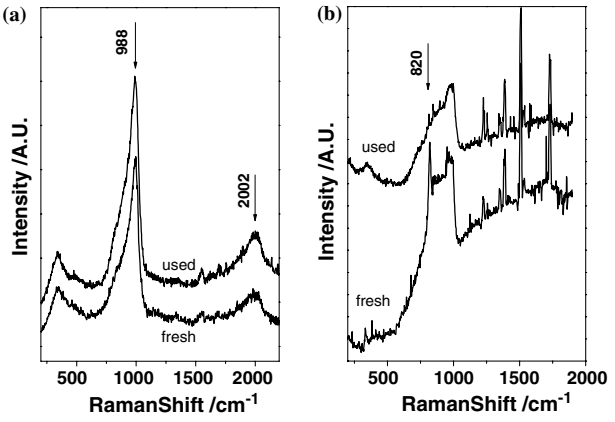

Figure 8. UV Raman [(a) λ_{ex} = 244 nm; (b) λ_{ex} = 325 nm)] of the fresh and used 8%Mo/MCM-22 catalysts.

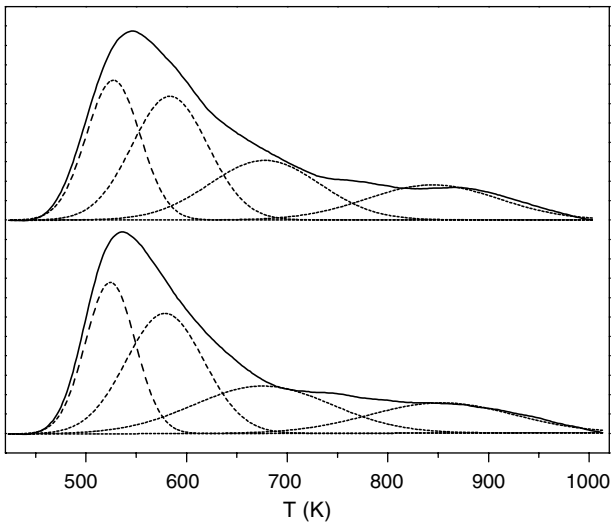

Figure 9. NH_3-TPD spectra: (a) fresh and (b) used 8%Mo/MCM-22 catalysts.

octahedral polyoxomolybdate Mo(VI) species was leached out during the reaction, while the isolated tetrahedral molybdate species remained almost unchanged.

NH_3-TPD technique was also applied to characterize the acidic sites of the fresh and used Mo/MCM-22 catalysts. Figure 9 and table 3 give the NH_3-TPD profiles and the corresponding curve fitting results of the fresh and used 8%Mo/MCM-22 catalyst, respectively. Based on the ascription of NH_3 desorption peak of Mo/MCM-22 by Shu *et al.* [18], it was found that the impregnated Mo species had interacted with the Brønsted acidic sites to generated the medium-strength acid sites. The results of the NH_3-TPD experiment also showed that there was little difference between the acidic properties of the fresh and used catalyst, suggesting that the acidic sites of Mo/MCM-22 did not change during the reaction, i.e., the leaching of the Mo species did not release the Brønsted acidic sites of HMCM-22, which were covered by Mo species in the preparation step. By combining with the above UV–Vis diffuse reflectance and UV Raman spectroscopy, the results of NH_3-TPD experiment implied that the interacteion between the polymolybdate octahedral Mo species and the MCM-22 zeolite was rather weak, while that between the isolated tetrahedral molybdate species and the MCM-22 zeolite was relatively strong.

3.5. The reactivity of different Mo species

Based on the above evidence, it is rather clear that the tetrahedral Mo species, chemically joined to the support surface, remained almost unchanged during the reaction, while the polymolybdate octahedral Mo species, which had a relatively weaker interaction with the MCM-22 zeolite, leached out during the reaction, especially at high Mo loading. Combining with the time-on-stream reaction data, in which HCHO remained unchanged, while the CO_x decreased during the reaction process, it is reasonable to suppose that the isolated tetrahedral molybdenum oxo-species was responsible for HCHO production, whilst the octahedral polyoxomolybdate species resulted in the total oxidation of methane. In order to confirm this speculation, the reaction data and the characterization results were further analyzed. In table 2, it can be found that the amount of polymolybdate octahedral Mo species decreased by about 33% for the 1%Mo/MCM-22 catalyst and 74% for the 8%Mo/MCM-22 catalyst. From the catalytic results, it can be seen that the space–time yield of CO_x decreased by 22% for the 1%Mo/MCM-22 catalyst and 70% for the 8%Mo/MCM-22 catalyst. The decrease in CO_x yield has a quantitatively correspondence with the decrease of the polymolybdate octahedral Mo species. It is not strange that the decrease of CO_x yield was less than that of the polymolybdate octahedral Mo species, especially for 1%Mo/MCM-22 catalyst, because the tetrahedral Mo species and the Brønsted acid sites of HMCM-22 (especially for 1%Mo/

Table 3
Peak temperatures of NH_3-TPD spectra and the corresponding amounts of acid sites of the fresh and used 8%Mo/MCM-22 catalysts

Sample	Peak 1		Peak 2		Peak 3		Peak 4	
	Peak temp. (K)	Area (a.u.)	Peak temp. (K)	Area (a.u.)	Peak temp. (K)	Area (a.u.)	Peak temp. (K)	Area (a.u.)
Fresh	525	4874	579	6042	675	4236	854	2800
Used	526	4856	583	6024	677	4221	845	2945

MCM-22) could also contribute to CO_x production. Over the tetrahedral Mo species, CO_x was a secondary product of HCHO oxidation due to the instability of the intermediate product, HCHO. Hence, the supposition mentioned above was further confirmed. It can also be concluded that the polymolybdate octahedral Mo species were more active for methane activation than the isolated tetrahedral Mo species, although the products were CO_x only.

In fact, the fresh and used Mo/MCM-22 catalysts in the present work could be considered as two catalysts having the same amount of tetrahedral Mo species, but different amount of polymolybdate octahedral Mo species. Thus, comparing with the previous investigations reported so far, this study gave more direct and convincing evidence for the correlation between the structure of the supported metal oxide phase and their role in the reaction mechanism.

4. Conclusion

Combining the characterization results of the fresh and the used Mo/HMCM-22 with the reaction data, correlation between the structure of the supported Mo species and their role in the reaction mechanism were explored more systematically and directly. By a series of systematic characterizations, it was shown that the tetrahedral Mo species chemically joined to the support surface remained almost unchanged during the reaction, while the polymolybdate octahedral Mo species, which had a relatively weaker interaction with the MCM-22 zeolite, leached out during the reaction, especially at high Mo loadings. The time-on-stream reaction data illustrated that HCHO yield remained unchanged, while the CO_x decreased during the reaction. And the decrease in CO_x yield has a quantitatively correspondence with the decrease of the polymolybdate octahedral Mo species. Thus, it can be concluded that the isolated tetrahedral molybdenum oxo-species (T_d) was responsible for HCHO production, while the octahedral polyoxomolybdate species (O_h) yielded the total oxidation product (CO_x).

Acknowledgments

Financial support from the Ministry of Science and Technology of China (National Key Project of Fundamental Research: G1999022406) is gratefully acknowledged.

References

[1] R. Pitchai and K. Klier, Catal. Rev.-Sci. Eng. 28 (1986) 13.
[2] R.H. Crabtree, Chem. Rev. 95 (1995) 987.
[3] T. Sugino, A. Kido, N. Azuma, A. Uedo and Y. Udagawa, J. Catal. 190 (2000) 118.
[4] R.G. Herman, Q. Sun, C. Shi, K. Klier, C.B. Wang, H. Hu, I.E. Wachs and M.M. Bhasin, Catal. Today 37 (1997) 1.
[5] S.H. Taylor, J.S.J. Hargreaves, G.J. Hutchings, R.W. Joyner and C.W. Lembacher, Catal. Today 42 (1998) 217.
[6] H. Berndt, A. Martin, A. Brückner, E. Schreier, D. Müllller, H. Kosslick, G.-U. Wolf and B. Lücke, J. Catal. 191 (2000) 384.
[7] M.R. Smith and U.S. Ozkan, J. Catal. 141 (1993) 124.
[8] M.A. Bañares, J.L.G. Fierro and J.B. Moffat, J. Catal. 142 (1993) 406.
[9] K. Aoki, M. Ohmae, T. Nanba, K. Takeishi, N. Azuma, A. Ueno, H. Ohfune, H. Hayashi and Y. Udagawa, Catal. Today 45 (1998) 29.
[10] A. de Lucas, J.L. Valverde, L. Rodriguezl, P. Sanchez and M.T. Garcia, Appl. Catal. A 203 (2000) 81.
[11] H.-F. Liu, R.-S. Liu, K.Y. Liew, R.F. Johnson and J.H. Lunsford, J. Am. Chem. Soc. 106 (1984) 4117.
[12] S. Irusta, E.A. Lombardo and E.E. Miró, Catal. Lett. 29 (1994) 339.
[13] T. Takemoto, K. Tabata, Y. Teng, L. Dai and E. Suzuki, Catal. Today 71 (2001) 47.
[14] N.D. Spencer, J. Catal. 109 (1988) 187.
[15] S. Kasztelan and J.B. Moffat, J. Chem. Soc., Chem. Commun. (1987) 1663.
[16] K. Vikulov, G. Martra, S. Coluccia, D. Miceli, F. Arena, A. Parmaliana and E. Paukshtis, Catal. Lett. 37 (1996) 235.
[17] M.R. Smith, L. Zhang, S.A. Driscoll and U.S. Ozkan, Catal. Lett. 19 (1993) 1.
[18] Y. Shu, D. Ma, L. Xu, Y. Xu and X. Bao, Catal. Lett. 70 (2000) 67.
[19] H. Liu, L. Su, H. Wang, W. Shen, X. Bao and Y. Xu, Appl. Catal. A 236 (2002) 263.
[20] D. Ma, D. Wang, L. Su, Y. Shu, Y. Xu and X. Bao, J. Catal. 208 (2002) 260, and references therein.
[21] M. Rubin and P. Chu, *US Patent 4,954,325* (1990).
[22] A. Corma, C. Corell and J. Pérez-Pariente, Zeolites 15 (1995) 2.
[23] N. Kumar and L. Lindfors, Appl. Catal. A 147 (1996) 175.
[24] A. Corma, C. Corell, J. Pérez-Pariente, J. Guil, R. Guil-Lopez, S. Nicolopoulus, J. Gonzalez-Calbet and M. Vallet-Regi, Zeolites 16 (1996) 7.
[25] L. Chen, L. Lin, Z. Xu, X. Li and T. Zhang, J. Catal. 157 (1995) 190.
[26] M.A. Bañares and J.L.G. Fierro, Catal. Lett. 17 (1993) 205.
[27] C.C. Williams, J.G. Ekerdt, J. Jehng, F.D. Hardcastle, A.M. Turek and I.E. Wachs, J. Phys. Chem. 95 (1991) 8781.
[28] C.C. Williams, J.G. Ekerdt, J. Jehng, F.D. Hardcastle, A.M. Turek and I.E. Wachs, J. Phys. Chem. 95 (1991) 8791.
[29] K. Segawa and W. Hall, J. Catal. 76 (1982) 133.
[30] G. Xiong, Z. Feng, J. Li, Q. Yang, P. Ying, Q. Xin and C. Li, J. Phys. Chem. B 104 (2000) 3581.